Scripta Materialia 265 (2025) 116728

Contents lists available at ScienceDirect

Scripta Materialia

journal homepage: www.journals.elsevier.com/scripta-materialia

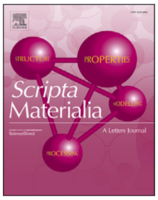

Analysis of correlations between intrinsic ductility and electronic density of states in refractory alloys

Amit Samanta [a,*], Michael Widom [b], Joel Berry [a], Aurélien Perron [a], Joseph McKeown [a]

[a] Lawrence Livermore National Laboratory, Livermore, CA 94550, USA
[b] Department of Physics, Carnegie Mellon University, Pittsburgh, PA 15213, USA

ABSTRACT

High entropy alloys (HEAs) correspond to a new and emerging class of materials that allows us to explore a large composition space to tune mechanical strength and thermal stability. Therefore, to design better alloys, it is important to scan the high-dimensional space of chemistry, composition and temperature. To facilitate this search, we present a method to screen intrinsically ductile body centered cubic (BCC) refractory alloys from electronic structure calculations by using the density of states (DOS) at the Fermi level, $g\left(\mu_F\right)$. This correlation between intrinsic ductility and $g\left(\mu_F\right)$ is tested by analyzing group V (V, Nb, Ta) and VI (Mo, W) refractory metals, binary alloys, such as W-Nb, W-V, Mo-Nb and Mo-V, and refractory alloys for which experimental stress-strain measurements are available. In addition, we perform a high-throughput exploration of the entire composition space of a recently proposed alloy system, CrMoNbV, and identify compositions that exhibit high intrinsic ductility.

Alloys for high temperature structural applications have traditionally been designed by starting with one or two principal elements and adding other elements in dilute concentrations to systematically tune the mechanical strength, thermal stability, and corrosion and oxidation resistance [5,14,23]. However, complex concentrated alloys (CCAs) and high entropy alloys (HEAs) correspond to a new and emerging class of materials that allows us to explore a significantly larger composition space to tune the properties [18,29,30]. In the past few years, researchers have predominantly focused on designing alloys in which the constituent elements form solid-solutions, resulting in single-phase microstructures that are thermodynamically stable at high temperatures (i.e., temperatures more than one-third of the melting point) to potentially replace Ni- or Co-base alloys for high temperature structural applications [22,24,35]. To this end, an exponentially growing list of alloys containing refractory metals (such as Nb, Ta, Cr, Mo, W) has been proposed in the literature [1]. However, a systematic exploration of the high-dimensional space of chemistry (i.e., search for potential alloying elements), composition and temperature to search for alloys (in which the solid solution phase is stable) is difficult, time consuming and resource intensive. In addition, the effect of short-range order (SRO) and segregation of alloying elements even in these specifically designed alloys can be detrimental to mechanical properties [20] and are often difficult to study using experiments due to slow diffusion and phase transition kinetics in these refractory alloys [33]. In the past few years researchers have used cluster expansion models, machine learning interatomic potentials and CALPHAD (CALculation of PHAse Diagrams) to perform high throughput analysis of phase stability [6,7,43] However, high-throughput screening of alloys with enhanced mechanical strength and ductility remains an open and challenging problem.

Among the body-centered cubic (BCC) refractory metals, the metals in group VI, i.e., Cr, Mo and W, exhibit low ductility and are usually associated with cleavage failure. On the other hand, metals in group V of the periodic table, i.e., V, Nb and Ta, have high ductility. A summary of fracture strains reported in the literature is shown in Table 1. Ductility is a macroscopic property of a material and depends on test conditions, dislocation density, dislocation mobility, dislocation nucleation and multiplication rates, chemistry and concentration of solute atoms, impurities like oxygen, nitrogen, etc., grain size, strain rate, temperature [10]. Some of these properties, such as dislocation mobility, ease with which dislocations nucleate and multiply, interactions between solute and impurity atoms with dislocations, stacking faults and grain boundaries are intrinsically determined by the electronic structure of a material. Note that macroscopic effects cannot be handled in routine electronic structure calculations which are performed with systems containing only a few hundred atoms. Therefore, the underlying assumption is that for sufficiently pure and well-annealed samples with large grain sizes, the effect of prior mechanical deformation and impurities can be minimized, and for such samples, fracture strain is strongly correlated

---

* Corresponding author.
E-mail address: samanta1@llnl.gov (A. Samanta).

https://doi.org/10.1016/j.scriptamat.2025.116728
Received 30 August 2024; Received in revised form 29 January 2025; Accepted 21 April 2025

Table 1
Comparison of electronic density of states at the Fermi level, $g\left(\mu_{\mathrm{F}}\right)$ (in states/eV/atom), obtained from density functional theory calculations and % elongation (near room temperature) for BCC refractory metals and high entropy alloys reported in the literature. The intrinsic ductility parameter [40] based on nonlinear elasticity theory is shown in brackets along with $g\left(\mu_{\mathrm{F}}\right)$. DFT calculations for alloys (solid solution phase) were performed using supercells containing 250 atoms and calculations for pure metals were performed by using conventional unit cells, each containing 2 atoms.

Alloy	$g\left(\mu_{\mathrm{F}}\right)$	% elongation
W	0.448 (0.78)	2 [40]
Mo	0.520 (0.88)	5-25 [40]
Ta	1.354 (3.84)	30-50 [4,40]
Nb	1.495 (2.52)	30-50 [3,40,41]
V	1.976 (3.49)	35-60 [3,40]
$Al_{1.00}$MoNbTiV	1.087	3 [1]
$Al_{0.75}$MoNbTiV	1.157	8 [1]
$Al_{0.50}$MoNbTiV	1.216	11 [1]
MoNbTaW	0.976	2.60 [11]
CrMoNbV	0.807	6 [8]
MoNbTaVW	1.162 (0.60)	1.70 [11]
MoNbTaTiW	1.196	14.1 [11]
NbTaVW	1.204 (1.29)	14 [42]
MoNbTaV	1.231	21 [42]
Hf24Nb23Ti38V15	1.365	22 [39]
HfNbTiVZr	1.397 (1.07)	30
HfNbTiV	1.500	15 [39]
NbTaTiV	1.670 (1.38)	40
Al25Hf25Nb25Ti25	1.09	<5 [25]
Al10Hf20Nb22Ti33V3	1.37	>40 [25]

with intrinsic ductility of the material. In other words, microstructural effects, such as grain size modulations, can be used to further enhance the ductility of an intrinsically ductile alloy but cannot transform an intrinsically brittle alloy into a ductile alloy.

Consequently, several approaches to identify or screen ductile alloys directly from physical properties obtained via ab initio calculations have been proposed in the literature [2]. For example, by using the Rice-Thompson parameter, Geller et al. hypothesized that metals which are stable in HCP crystal structure can weaken Mo against shear in the (110) plane [10]. From first principles calculations, Medvedeva et al. observed that change in chemical bonding upon addition of solute atoms to Mo decreases the stacking fault energy (SFE) and enhances the nucleation of double-kinks and dislocation mobility, which the authors were able to relate to increase in free electrons (upon addition of solute atoms) and filling of anti-bonding states [16,21]. Further, Medvedeva et al., in Ref. [17], reported a close correlation between change in core structure of screw dislocations upon inclusion of solutes in Mo to solutes (Re, Os, Ir, Pt) that decrease the SFE of Mo. These conclusions are in line with calculations performed by Romaner et al. which suggest that doping W with Re decreases the Peierls energy barrier and changes the core structure of screw dislocations and the preferred slip plane [27]. Using electronic structure calculations, Qi et al. demonstrated that alloying Mo and W with group IV and V elements can enhance intrinsic ductility because they induce shear failure under tension [19,26]. The authors further demonstrated that the transition from cleavage to shear failure is closely related to changes in the band structure and Fermi level, μ_{F}, under stress. The picture emerging from these seemingly different analyses is that the inclusion of some solute atoms in Mo or W leads to decrease in SFE, Peierls barrier and dislocation core structure and changes in these physical properties are closely related to increase in free electrons and change in Fermi level [12]. Even though each of these methods for enhancing intrinsic ductility is theoretically promising, in practice, the large statistical uncertainty in experimental measurements of fracture strain makes it difficult to assess and rank the robustness of these ideas in screening alloys. Recently, Wang et al. [38] demonstrated a strong correlation exists between the core structure of screw dislocations, Peierls energy barrier and dislocation nucleation barrier in binary alloys of W and Mo, and proposed the χ parameter to identify intrinsically ductile alloys. This parameter is calculated from $\chi=\Delta E^{a} / \Delta E^{p}$ where $\Delta E=E_{\mathrm{FCC}}-E_{\mathrm{BCC}}$ and superscripts a and p represent alloy or pure BCC metals, respectively. Even though χ is able to identify intrinsically ductile binary alloys but its generalization to CCAs or HEAs is not straightforward.

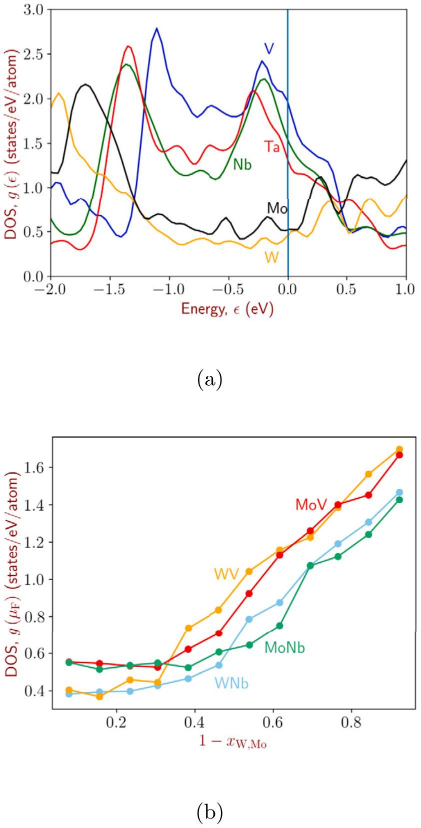

(a)

(b)

Fig. 1. (a) Comparison of electronic density of states for different BCC metals close to the Fermi level. The Fermi level is at 0 eV. Within a rigid band model, change in DOS at μ_{F} is closely related to the number of valence electrons [25]. (b) Density of states at the Fermi level for Mo-V, Mo-Nb, W-V and W-Nb binary alloys.

Recently, Winter et al. proposed the intrinsic ductility parameter, which is based on nonlinear elasticity theory and allows for screening of alloys based on shear instability [40]. Even though this intrinsic ductility parameter can differentiate between ductile and brittle BCC metals and alloys, the use of higher order elastic constants makes this procedure computationally expensive [3,32,41]. In this work, we explore correlations between intrinsic ductility of a refractory alloy and the electronic density of states at the Fermi level, $g\left(\mu_{\mathrm{F}}\right)$, and assess the viability of using $g\left(\mu_{\mathrm{F}}\right)$ to efficiently identify intrinsically ductile alloys. While this work is motivated by the systematic analysis of Cr-V alloys performed by Gao et al. [9] and analysis of solute-defect interactions by Yong et al. [13], we note that correlations between intrinsic ductility and DOS were also conjectured by Geller at el. [10], Samolyuk et al. [28] and Hu et al. [13] but a systematic validation of this correlation has not been reported in the literature.

To understand the correlation between ductility and the electronic density of states, the calculated density of states for BCC refractory metals is shown in Fig. 1a. The DOS curves are shifted such that the Fermi level is positioned at 0 eV. For Mo and W, in agreement with prior literature, the Fermi level lies in a pseudo-gap between the bonding and anti-bonding d-states [9,10,28]. The group V refractory metals (V, Nb, Ta) which occupy the same column of the periodic table have 5 valence electrons shared between the d- and s-states. Consequently, the pseudogaps in these three metals lie to the left of the Fermi level and these metals have high DOS at the Fermi level [10]. The DOS at the Fermi level listed in Table 1 shows a clear difference between group VI elements, Mo and W, for which $g\left(\mu_{\mathrm{F}}\right) < 0.60$ states/eV/atom and group V elements, Ta, Nb and V, for which $g\left(\mu_{\mathrm{F}}\right) > 1.30$ states/eV/atom.

The sharp differences in $g\left(\mu_{\mathrm{F}}\right)$ values for Mo and W compared to V, Nb, and Ta coincide with the large differences in their % elongation values reported in the literature. Electronic structure calculations for chromium, which is another group VI metal of the periodic table, show that $g\left(\mu_{\mathrm{F}}\right) = 0.738$ states/eV/atom. Chromium is particularly attractive for high-temperature structural material due to its good thermal shock resistance, and superior oxidation resistance as compared to the other refractory metals, but has low ductility [34,36]. Here we note that mechanical properties of niobium and vanadium are very sensitive to test conditions, such as temperature, strain rate, concentration of impurities and solute atoms, and atmosphere conditions. Impurities and miscible solute atoms in Nb and V, even if present in small amount, easily trap dislocations which leads to strain aging and intermittent yielding [3]. This results in significant variations in the tensile strength and ductility [3,32,41]. Even after accounting for these variations in strength and fracture strain measurements, there is a noticeable gap in the mechanical response of group V and group VI elements and this coincides with the differences in their $g\left(\mu_{\mathrm{F}}\right)$ values. This suggests that $g\left(\mu_{\mathrm{F}}\right)$ can be used to separate intrinsically ductile metals from intrinsically brittle metals.

Next, to explore if a similar correlation exists between intrinsic ductility and the $g\left(\mu_{\mathrm{F}}\right)$ in alloys, in Fig. 1b we show the electronic DOS of four binary alloy systems – Mo-Nb, Mo-V, W-Nb and W-V. To obtain the density of states, first, structural optimizations were performed using supercells containing 128 atoms to obtain the equilibrium supercell dimensions for each composition. Next, the electronic DOS was calculated from a separate simulation. For W-Nb and W-V, $g\left(\mu_{\mathrm{F}}\right)$ is close to that of pure W (see Table 1) in the tungsten-rich limit. Similarly, in the Nb- or V-rich limit, $g\left(\mu_{\mathrm{F}}\right)$ is close to DOS at Fermi level for pure Nb and V, respectively. A similar trend is evident for Mo-Nb and Mo-V alloys. Interestingly, for both Mo and W binary alloys, $g\left(\mu_{\mathrm{F}}\right)$ is almost constant between 60-100% concentrations of Mo and 70-100% concentrations of W which suggests that small concentrations of Nb and V are not sufficient to change the fracture strains in Mo and W. In Fig. 1b, $g\left(\mu_{\mathrm{F}}\right)$ increases monotonically and converges to that of pure Nb or pure V as the concentration of Mo and W decreases. To the best our knowledge, tensile test results for different binary systems (W-V, W-Nb, Mo-V, Mo-Nb) are not available in the literature. Hence, to assess correlations between intrinsic ductility and $g\left(\mu_{\mathrm{F}}\right)$, we have compared with the χ parameter [38]: The increase in $g\left(\mu_{\mathrm{F}}\right)$ for higher Nb and V concentrations is in line with the decrease in χ when V concentration is higher than ∼35% in W-V alloys and Nb concentration is higher than ∼25% in W-Nb alloys.

In principle, to minimize statistical errors, many different distributions of elements on the BCC lattice must be considered for each composition. But our results show that statistical errors associated with different elemental distributions are typically less than 0.05 states/eV/atom which is smaller than changes in $g\left(\mu_{\mathrm{F}}\right)$ observed in Fig. 1b. In addition, $g\left(\mu_{\mathrm{F}}\right)$ is insensitive to changes in supercell dimensions (up to 2% hydrostatic strains for Mo-V, Mo-Nb, W-V and W-Nb binary alloys). However, physical properties used in other metrics to identify intrinsically ductile alloys, such as shear moduli, SFE and Perierls barrier, are sensitive to small changes in the lattice parameter.

Figure 1b suggests that V has a stronger effect on the intrinsic ductility of Mo and W than Nb. Since the FCC phase is unstable in some of the binary alloys, using unrelaxed structures we found that the material index χ [38] reaches a maximum at ∼70% and ∼80% Mo concentrations in Mo-V and Mo-Nb alloys, respectively, and decreases monotonically with decrease in Mo concentration. In W-V alloys, the material index χ monotonically decreases even for small concentrations of V, but in W-Nb alloys, χ reaches a maximum at ∼80% W and decreases thereafter with increase in Nb concentration. However, these results are in contrast to the predictions obtained by Wang et al. [38] which suggests that Nb has a stronger effect on the intrinsic ductility of Mo and W. We attribute this discrepancy to changes in χ due to local strain effects or structural distortions when the BCC phase is unstable. This highlights another advantage of using $g\left(\mu_{\mathrm{F}}\right)$: For the four binary systems in Fig. 1b, changes in $g\left(\mu_{\mathrm{F}}\right)$ due to atomic relaxations are also smaller than 0.05 states/eV/atom. This highlights the importance of chemical/electronic effects to $g\left(\mu_{\mathrm{F}}\right)$ than local relaxations as has also been highlighted by Yong et al. [13].

To provide further evidence of the strong correlation between $g\left(\mu_{\mathrm{F}}\right)$ and % elongation, we analyzed high entropy alloys for which tensile or compression tests have been reported in the literature. Experiments performed on Al doped MoNbTiV suggest that increase in Al leads to a decrease in ductility. This trend agrees with DFT calculations of $g\left(\mu_{\mathrm{F}}\right)$ (see Table 1) which decreases from 1.216 to 1.087 states/eV/atom with increase in Al concentration. According to the results in Table 1, two other alloys that have low ductility are MoNbTaW and MoNbTaVW and $g\left(\mu_{\mathrm{F}}\right)$ obtained from DFT calculations are 0.976 and 1.162 states/eV/atom. On the other hand, compression experiments performed on NbTaVW and MoNbTaTiW show nearly 14% deformation before fracture. Surprisingly, even though $g\left(\mu_{\mathrm{F}}\right)$ for W and Mo are close, replacing W in NbTaVW with Mo increases $g\left(\mu_{\mathrm{F}}\right)$ from 1.204 to 1.231 states/eV/atom. The resulting alloy, MoNbTaV, has higher ductility than NbTaVW. If W is replaced with Ti, then the DOS at the Fermi level for resulting alloy (NbTaTiV) is 1.670 and the reported % elongation is close to that of pure Nb and V. These results suggest that $g\left(\mu_{\mathrm{F}}\right) \approx 1.20$ states/eV/atom can be used to separate ductile alloys from their brittle counterparts.

High-throughput exploration of composition space of Cr-Mo-Nb-V: The equiatomic CrMoNbV alloy proposed by Feng et al. [8] and Lee et al. [15] has generated a lot of excitement in the past few years due to

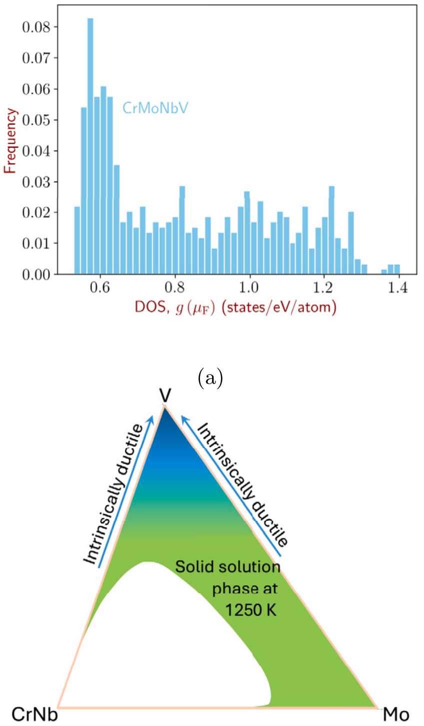

(a)

(b)

Fig. 2. (a) The distributions of density of states at the respective Fermi levels, $g\left(\mu_{\mathrm{F}}\right)$ for sampled compositions in the Cr-Mo-Nb-V alloy system obtained from high-throughput DFT calculations. (b) Compositions corresponding to intrinsically ductile (solid solution) alloys are highlighted on the Cr-Mo-Nb-V phase diagram at 1250 K obtained from CALPHAD in Ref. [43]. Compositions with $g\left(\mu_{\mathrm{F}}\right) < 1.20$ are shown in green.

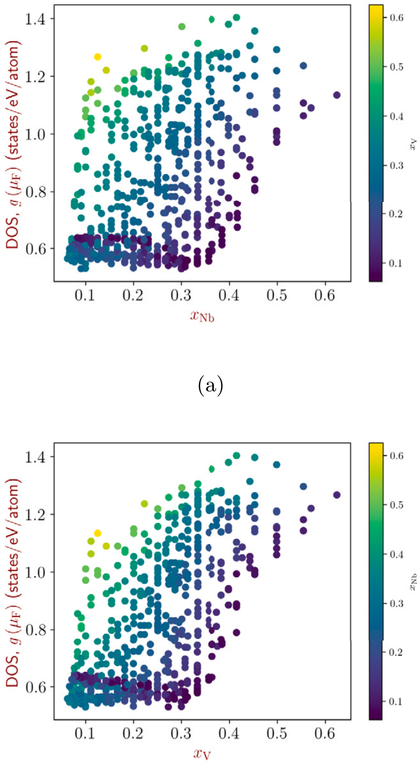

(a)

(b)

Fig. 3. The distribution of density of states at the Fermi level, $g(\mu_F)$ for 591 compositions in the Cr-Mo-Nb-V system obtained from high-throughput DFT calculations. The color-bar shows the fraction of V atoms in (a) and Nb atoms in (b).

its remarkably high tensile strength of ∼2 GPa and ductility of 15% at 1173 K. This interest can be attributed to the fact that most conventional superalloys and HEAs reported in the literature experience a significant reduction in mechanical strength above 1200 K [15,31]. In contrast to strengthening due to obstruction of dislocations at interfaces between the matrix and precipitates, the high tensile strength and ductility in CrMoNbV has been attributed to large atomic size mismatch, variations in elastic constants of constituent elements and to pinning of non-screw type dislocations.

To design alloys with high intrinsic ductility, it is important to explore the whole composition space and identify promising candidates. To this end, we performed a high throughput exploration (see Supplementary Materials) of the whole composition space to search alloys with high density of states at the Fermi level and the results are summarized in Figs. 2a and 3. As shown in Fig. 2, for all compositions considered in this study, $g(\mu_F)$ lies between 0.4 and 1.4 states/eV/atom which covers the range of values obtained for the constituent elements in Table 1 and Fig. 1a. Alloys with $g(\mu_F)$ around 0.4 (see Fig. 3) correspond to high Mo concentration and those with $g(\mu_F) > 1.2$ states/eV/atom correspond to alloys with higher Nb or V concentrations.

In Refs. [33,43], using cluster expansion models, CALPHAD calculations and experiments, it was concluded that solid solution phase does not touch the Cr-Nb edge of the quaternary phase diagram but exists close to the Mo-V and Nb-V edges at high temperatures (see Fig. 2b). For example, the solid solution phase was found to be stable in $(Mo_{0.50}Nb_{0.50})_x(Cr_{0.50}V_{0.50})_{(1-x)}$ for $x < 0.09$ and $x > 0.91$. Similarly, in $(Cr_{0.50}Nb_{0.50})_y(Mo_{0.50}V_{0.50})_{(1-y)}$, the solid solution phase was found to be stable for $y < 0.29$. Hence, for thermodynamic stability of the solid solution phase, alloys with high Nb concentration are not good candidates. On the other hand, Cr and Mo are detrimental to the intrinsic ductility of an alloy, yet are important for oxidation resistance and high melting point, respectively. Therefore, the best strategy is to use alloys with higher V concentration, which is in line with conclusions obtained from recent experiments performed on V_xNbMoTa [37].

CRediT authorship contribution statement

Amit Samanta: Writing – review & editing, Writing – original draft, Methodology, Conceptualization. **Michael Widom:** Writing – review & editing, Conceptualization. **Joel Berry:** Writing – review & editing, Conceptualization. **Aurélien Perron:** Writing – review & editing, Resources, Conceptualization. **Joseph McKeown:** Writing – original draft, Resources, Funding acquisition, Conceptualization.

Declaration of competing interest

The authors declare that they have no known competing financial interests or personal relationships that could have appeared to influence the work reported in this paper.

Acknowledgements

This work was performed under the auspices of the U.S. Department of Energy by Lawrence Livermore National Laboratory under Contract DE-AC52-07NA27344. This work was funded by the Laboratory Directed Research and Development (LDRD) Program at LLNL under project tracking code 22-SI-007. M.W. was supported by DOE grant DE-SC0014506 for the electronic structure calculations of AlHfNbTiV alloys using randomized structures provided by Jie Qi. A. S. wishes to thank Liang Qi (University of Michigan) for his insightful comments on the manuscript. LLNL IM release number is LLNL-JRNL-868770.

Appendix. Supplementary material

Supplementary material related to this article can be found online at https://doi.org/10.1016/j.scriptamat.2025.116728.

References

[1] C.K. Borg, C. Frey, J. Moh, T.M. Pollock, S. Gorsse, D.B. Miracle, O.N. Senkov, B. Meredig, J.E. Saal, Sci. Data 7 (2020) 1.
[2] P.P. Borges, R.O. Ritchie, M. Asta, Sci. Adv. 10 (2024) eadp7670.
[3] V. Borisenko, V. Krashchenko, V. Statsenko, Strength Mater. 11 (1979) 89.
[4] T.S. Byun, S.A. Maloy, J. Nucl. Mater. 377 (2008) 72.
[5] J. Dai, J. Zhu, C. Chen, F. Weng, J. Alloys Compd. 685 (2016) 784.
[6] K.L. Elder, J. Berry, B. Bocklund, S.K. McCall, A. Perron, J.T. McKeown, npj Comput. Mater. 9 (2023) 84.
[7] K.L. Elder, J. Berry, A. Perron, B. Bocklund, J. Shittu, C.J. Rietema, H.B. Henderson, S.K. McCall, J.T. McKeown, npj Comput. Mater. 9 (2023) 88.
[8] R. Feng, B. Feng, M.C. Gao, C. Zhang, J.C. Neuefeind, J.D. Poplawsky, Y. Ren, K. An, M. Widom, P.K. Liaw, Adv. Mater. 33 (2021) 2102401.
[9] M.C. Gao, Y. Suzuki, H. Schweiger, Ö.N. Doğan, J. Hawk, M. Widom, J. Phys. Condens. Matter 25 (2013) 075402.
[10] C.B. Geller, R.W. Smith, J.E. Hack, P. Saxe, E. Wimmer, Scr. Mater. 52 (2005) 205.
[11] Z. Han, N. Chen, S. Zhao, L. Fan, G. Yang, Y. Shao, K. Yao, Intermetallics 84 (2017) 153.
[12] Y.-J. Hu, A. Sundar, S. Ogata, L. Qi, Acta Mater. 210 (2021) 116800.
[13] Y.-J. Hu, G. Zhao, B. Zhang, C. Yang, M. Zhang, Z.-K. Liu, X. Qian, L. Qi, Nat. Commun. 10 (2019) 4484.
[14] S. Jayasathyakawin, M. Ravichandran, N. Baskar, C.A. Chairman, R. Balasundaram, Mater. Today Proc. 27 (2020) 909.
[15] C. Lee, F. Maresca, R. Feng, Y. Chou, T. Ungar, M. Widom, K. An, J.D. Poplawsky, Y.-C. Chou, P.K. Liaw, et al., Nat. Commun. 12 (2021) 1.
[16] N. Medvedeva, Y.N. Gornostyrev, A.J. Freeman, Phys. Rev. Lett. 94 (2005) 136402.
[17] N. Medvedeva, Y.N. Gornostyrev, A.J. Freeman, Phys. Rev. B 72 (2005) 134107.
[18] D.B. Miracle, O.N. Senkov, Acta Mater. 122 (2017) 448.
[19] N. Nagasako, M. Jahnátek, R. Asahi, J. Hafner, Phys. Rev. B 81 (2010) 094108.
[20] C. Nataraj, E.J.L. Borda, A. van de Walle, A. Samanta, Acta Mater. 220 (2021) 117269.
[21] A.R. Natarajan, A. Van der Ven, npj Comput. Mater. 6 (2020) 80.
[22] J.H. Perepezko, Science 326 (2009) 1068.

[23] D.A. Porter, K.E. Easterling, Phase Transformations in Metals and Alloys, Chapman and Hall, London, 1992.
[24] S. Praveen, H.S. Kim, Adv. Eng. Mater. 20 (2018) 1700645.
[25] J. Qi, X. Fan, D.I. Hoyos, M. Widom, P.K. Liaw, J. Poon, Sci. Adv. 10 (2024) eadq0083.
[26] L. Qi, D. Chrzan, Phys. Rev. Lett. 112 (2014) 115503.
[27] L. Romaner, C. Ambrosch-Draxl, R. Pippan, Phys. Rev. Lett. 104 (2010) 195503.
[28] G.D. Samolyuk, Y. Osetsky, R. Stoller, J. Phys. Condens. Matter 25 (2013) 025403.
[29] O.N. Senkov, J.D. Miller, D.B. Miracle, C. Woodward, Nat. Commun. 6 (2015) 1.
[30] O.N. Senkov, G.B. Wilks, D.B. Miracle, C.P. Chuang, P.K. Liaw, Intermetallics 18 (2010) 1758.
[31] O.N. Senkov, G.B. Wilks, J.M. Scott, D.B. Miracle, Intermetallics 19 (2011) 698.
[32] S. Shi, L. Zhu, H. Zhang, Z. Sun, Mater. Lett. 189 (2017) 310.
[33] J. Shittu, C.J. Rietema, M. Juhasz, B. Ellyson, K.L. Elder, B.J. Bocklund, Z.C. Sims, T.T. Li, H.B. Henderson, J. Berry, et al., J. Alloys Compd. 977 (2024) 173349.
[34] J.R. Stephens, W.D. Klopp, Ductility mechanisms and superplasticity in chromium alloys, National Aeronautics and Space Administration, 1968.
[35] M.-H. Tsai, J.-W. Yeh, Mater. Res. Lett. 2 (2014) 107.
[36] R. Wadsack, R. Pippan, B. Schedler, J. Nucl. Mater. 307 (2002) 701.
[37] M. Wang, Z. Ma, Z. Xu, X. Cheng, Mater. Sci. Eng. A 808 (2021) 140848.
[38] R. Wang, L. Zhu, S. Pattamatta, D.J. Srolovitz, Z. Wu, Mater. Today 79 (2024) 36.
[39] S. Wei, S.J. Kim, J. Kang, Y. Zhang, Y. Zhang, T. Furuhara, E.S. Park, C.C. Tasan, Nat. Mater. 19 (2020) 1175.
[40] I. Winter, M. de Jong, J. Montoya, E. Rothchild, D. Chrzan, Phys. Rev. Mater. 3 (2019) 113608.
[41] G. Wu, N. Dhanaraj, L. Cooley, D. Hicks, E. Hahn, D. Burk, W. Muranyi, M. Foley, H. Edwards, E. Harms, et al., in: AIP Conference Proceedings, vol. 1218, American Institute of Physics, 2010, pp. 857–862.
[42] H. Yao, J. Qiao, J. Hawk, H. Zhou, M. Chen, M. Gao, J. Alloys Compd. 696 (2017) 1139.
[43] S. Zhu, J. Shittu, A. Perron, C. Nataraj, J. Berry, J.T. McKeown, A. van de Walle, A. Samanta, Acta Mater. 255 (2023) 119062.